Vibrational damping properties of finite microperforated plates

Lucie Gallerand [1]
École de technologie supérieure
Montréal, Canada

Mathias Legrand
McGill University
Montréal, Canada

Thomas Dupont
École de technologie supérieure
Montréal, Canada

Philippe Leclaire
Université de Bougogne
Nevers, France

ABSTRACT

Microperforated plates (MPP) are traditionally used in sound control technologies to advantageously absorb acoustic waves. However, little is known concerning the additional structural damping they can induce through exchanges in the viscous and thermal boundary layers near the fluid-structure interface of the microperforations. MPP therefore offer an alternative to, or can be used together with, viscoelastic materials, commonly implemented to damp vibrations at medium and high frequencies. In this work, the structural damping capabilities of finite MPP are investigated. First, an analytical model is developed using an alternative form of the Biot model, classically devoted to porous plates, involving energy dissipation through viscous friction mechanisms. The analytical results are compared to experimental measurements of structural damping factors on various MPP samples. The model is validated and confirms the damping effect added by the microperforations in the low frequency range. A sensitivity analysis on perforation rate and perforation diameter provides a characteristic frequency that when coinciding with a plate natural frequency maximizes the added damping.

1. INTRODUCTION

Over the last few decades, microperforated plates (MPP) have been used as lightweight sound absorbers mainly because of their environment-friendly and hygienic properties. These simple structures can be made of various materials depending on the sought features: translucent (plexiglass), resistant to hostile environments (aluminum, steel, ...), biodegradable (wood, ...). These versatile sound absorption technologies are implemented, for instance, in cooling systems for turbines or in sound environments

[1] lucie.gallerand.1@ens.etsmtl.ca

targeting comfort. These structures are known to dissipate acoustic energy as heat through exchanges in the viscous and thermal boundary layers near the fluid-solid interface of the microperforations. Multiple theoretical approaches have been developed to characterize the absorption coefficient of MPP. In this acoustic context, microperforated plates have been modelled by Maa [1] using Kirchhoff's equations. Maa's work has been extended in a vibroacoustic context where MPP acoustic properties have been also investigated in the light of structural vibration [2, 3, 4]. However, the contribution of the microperforated plate to vibration damping is generally neglected.

The structural dynamics of porous plates was concurrently explored using an alternative form of Biot's theory of poroelasticity [5, 6] leading to complicated equations. A simpler model in the form of two coupled partial differential equations governing the dynamics of a finite-size porous plate was proposed [7]. In this work, it showed that the porous plate induces additional damping at a characteristic frequency which is only function of porous plate geometrical parameters and fluid characteristics. Furthermore, an equivalent fluid concept already derived in for porous systems, was used in [8] for a sufficiently rigid structure to characterize acoustic proprertis of MPP. It has also been reported that fluid-solid interactions and visco-thermal effects induce additional damping in the case of MPP [9]. However, this effect has never been explored in detail.

The present work suggests to identify a finite size MPP to a porous plate with the aim of deriving an analytical model able to capture the additional damping features of MPP. In the first section, the analytical model is explained. The second section introduces the measurement procedure and corresponding results. Validation of the model is undertaken in a third section and closing comments are provided in the fourth and last section. The approaches and analyses proposed in the remainder are thoroughly developed in [10], available in Open Access.

2. STRUCTURAL DYNAMIC OF FINITE-SIZE MPP

2.1. Analytical model

In this work, the microperforations have a circular cross-section of diameter d constant over the thickness h of the plate. By identifying the MPP, of dimensions $L_x \times L_y \times h$, to a porous plate, a model developed in the context of the vibration analysis of porous plates [7] is adapted to MPP. Bending only is considered and the MPP is regarded as a homogeneous plate excited by an external load $f_{\text{ext}}(x, y, t)$. The dynamic response of a MPP whose perforations are fluid-saturated is solution to the two coupled equations

$$\Big(D + \frac{\alpha^2 M_\text{f} h^3}{12}\Big)\nabla^4 w_\text{s}(x,y,t) + h(\rho \ddot{w}_\text{s}(x,y,t) + \rho_\text{f}\ddot{w}(x,y,t)) = f_{\text{ext}}(x,y,t), \tag{1a}$$

$$\alpha M_\text{f}\nabla^2 w_\text{s}(x,y,t) - \rho_\text{f}\ddot{w}_\text{s}(x,y,t) - m(j\omega)\ddot{w}(x,y,t) = 0. \tag{1b}$$

Equation (1a) represents the elastic response of the homogeneous plate and Equation (1b) corresponds to the relative fluid-solid motion where $\nabla^4(\cdot) = \nabla^2(\cdot)^2$ and $\nabla^2(\cdot) = \frac{\partial^2(\cdot)}{\partial x^2} + \frac{\partial^2(\cdot)}{\partial y^2}$ and $w(x,y,t) = \phi(w_\text{f}(x,y,t) - w_\text{s}(x,y,t))$ with $w_\text{f}(x,y,t)$ is the fluid displacements and $w_\text{s}(x,y,t)$ the solid displacements. The parameters α and M_f are elastic coefficients defined by Biot [11]. The coefficient D is the bending stiffness and the friction in the boundary layers in the perforations is represented by the complex coefficient

$$m(j\omega) = \frac{1}{\phi}\Big(\rho_\text{f}\alpha_\infty + \frac{\sigma\phi}{j\omega}\Big), \tag{2}$$

where ρ_f is the fluid density. The above definition of $m(j\omega)$ is only effective valid in the low frequency range. Moreover, the parameters in the Biot theory (resistivity to airflow σ, perforation rate ϕ and tortuosity α_∞) are adapted to the particular case of MPP and listed in Table 1. Note that acoustic radiation in the perforation is considered in α_∞ through the parameter $\varepsilon = 0.24\sqrt{\pi d^2}(1 - 1.14\sqrt{\phi})$ [8]. In Table 1, N_perf is the number of microperforations and μ_f is the dynamic viscoelasticity of the fluid. In addition, the mechanical parameters of the MPP (Young's modulus and solid mass density)

Table 1: Geometrical parameter of a porous material adapted to MPP.

Airflow resistivity	Perforated rate	Tortuosity
$\sigma = \frac{32\mu_f}{\phi d^2}$	$\phi = \frac{N_{perf}\pi d^2}{4L_xL_y}$	$\alpha_\infty = 1 + \frac{2\varepsilon}{h}$

are also adapted to take account of perforations. Equivalent mechanical parameters are therefore defined [10, 12] as function of perforation diameter such that

$$E(\phi) = E\frac{(1-\phi^2)}{1+(2-3\nu)\phi}, \tag{3a}$$

$$\rho_s(\phi) = \rho_s(1-\phi), \tag{3b}$$

where E, ρ_s and ν are respectively the Young's modulus, the solid density and the Poisson's coefficent of a non-perforated plate.

2.2. Characteristic frequency and maximum damping

The external load is set to zero and a modal analysis is performed to solve Equation (1) from which modal damping factors and the natural frequencies are readily obtained. An equivalent forced-response analysis is provided in [10].

In the context of porous plate, a characteristic frequency f_c is defined by Leclaire *et al.* [7] based on Biot's frequency. This frequency is characteristic of the viscous frictions between the fluid and the solid and depends only on the geometry of the porous materials and the parameters of the fluid. At f_c, the additional damping induced by visco-thermic dissipation in the pores reaches a maximum [7]. By using MPP geometrical parameters defined in Table 1, the characteristic frequency is adapted to MPP as a function of d:

$$f_c(d) = \frac{32\mu_f}{2\pi\alpha_\infty\rho_f d^2}. \tag{4}$$

In the following, MPP are made of aluminum and their loss factor is fixed at 0.01 %. The global loss factors therefore include both the structural damping of aluminum and the additional damping induced by the microperforations. Moreover, the natural resonance frequencies consider the structural damping and the damping added by the microperforations.

In Figure 1, the loss factor for the first MPP mode is plotted as a function of the dimensionless frequency $f/f_c(d)$ for three different values of ϕ. For a finite-size MPP, the additional damping is

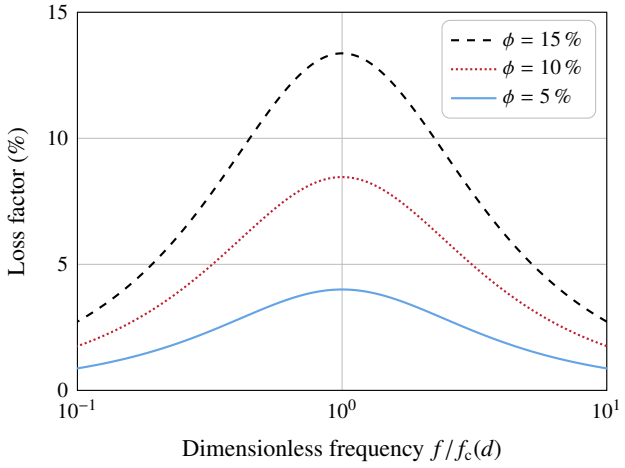

Figure 1: Global loss factor for the first MPP mode for three different values of ϕ. Perforation diameter d set to maximize the additional damping on the first resonance, such that $f_c(d) = f_{11}$.

maximum for the mode mn when $f_c(d)$ coincides with a resonance frequency f_{mn} where m and n are the indices of the modal discretization in the x and y directions. For a given ϕ, since the damping frequency is a function of d it is possible to adjust this last one to improve the damping capabilities of the MPP. Indeed, for a given mode there is a value of d for which the damping added by the microperforations is maximal. For a given ϕ, it appears in Figure 1 that the maximum damping is reached when there is coincidence between f_{11} and $f_c(d)$. In other words, the additional damping provided by the microperforations is largest at the characteristic frequency, but also acts over a range of frequencies around it, as shown by the envelope in terms of damping around $f/f_c(d) = 1$ in Figure 1. Moreover, for a given perforation diameter, the additional damping increases significantly with ϕ in Figure 1. The choice of ϕ is thus a compromise between the additional damping and the mechanical properties of the MPP since ϕ affects the natural frequencies by modifying the mass and the stiffness of the system.

In the following, the dimensions of the MPP along x and y are modified in order to explore the sensitivity of the first resonant frequency f_{11} to the additional damping. Two different MPP, denoted MPP1* and MPP1, with constant ϕ are considered. For both MPP, d is fixed to induce a maximum damping on the first mode so that $f_c(d_1^*) = f_{11}^* = 10\,\text{Hz}$ for MPP1* and $f_c(d_1) = f_{11} = 18\,\text{Hz}$ for MPP1. The corresponding loss factor is plotted as a function of dimensionless frequency in Figure 2. The

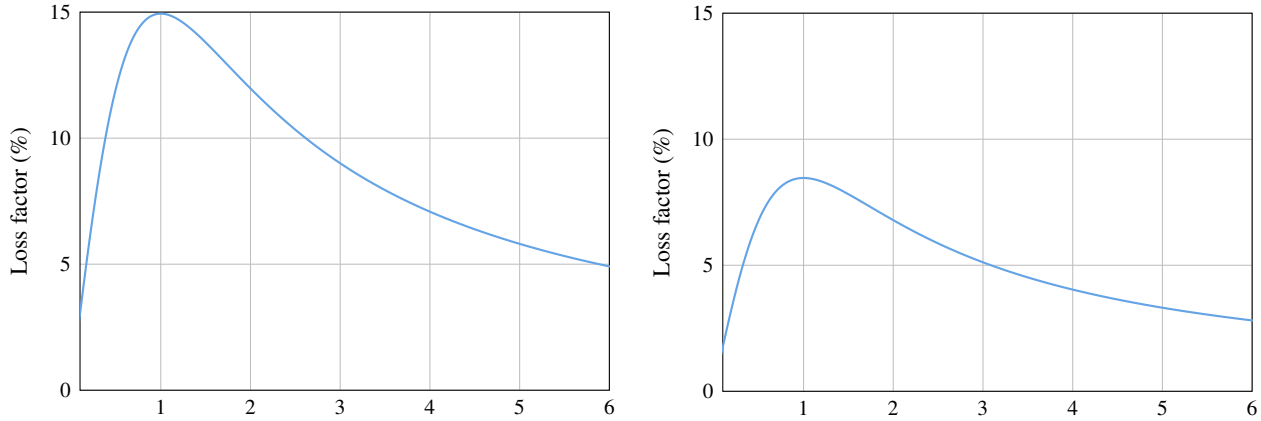

(a) $f_c(d_1^*) = 10\,\text{Hz}$ (b) $f_c(d_1) = 18\,\text{Hz}$

Figure 2: Global loss factor with constant $\phi = 10\,\%$: (a) MPP size is $490\,\text{mm} \times 570\,\text{mm} \times 1\,\text{mm}$, (b) MPP size is $700\,\text{mm} \times 700\,\text{mm} \times 1\,\text{mm}$. In (a) and (b), d is set to induce maximum additional damping on the first resonance mode.

comparison between MPP1* in Figure 2(a) and MPP1 in Figure 2(b) shows that the lower the natural frequency of the mode, the greater the damping added by the microperforations. This observation was confirmed numerically in many cases. The additional damping induced by the microperforations is therefore all the more important at low frequencies.

The influence of the considered vibration mode is now investigated. To this end, two MPP are considered. For the first one, denoted MPP1, the perforation diameter $d \equiv d_1$ is adjusted to induce maximum damping on the first vibration mode with natural frequency $f_c(d_1) = f_{11} = 18\,\text{Hz}$. For the second one, denoted MPP2, the perforation diameter $d \equiv d_2$ is adjusted to induce maximum damping on the second vibration mode with natural frequency $f_c(d_2) = f_{12} = 41\,\text{Hz}$. Their respective loss factor as a function of dimensionless frequency is illustrated in Figure 3. Both MPP share the same perforation rate $\phi = 10\,\%$ and plate dimensions. The comparison between Figure 3(a) and 3(b) shows that the maximum damping is observed for MPP1 and therefore for the first vibration mode.

With regard to Figure 2 and 3, a microperforated plate is show to feature more additional damping if f_c is in the low frequency range. It is therefore recommended to quantify d so as to have $f_c(d) = f_{11}$

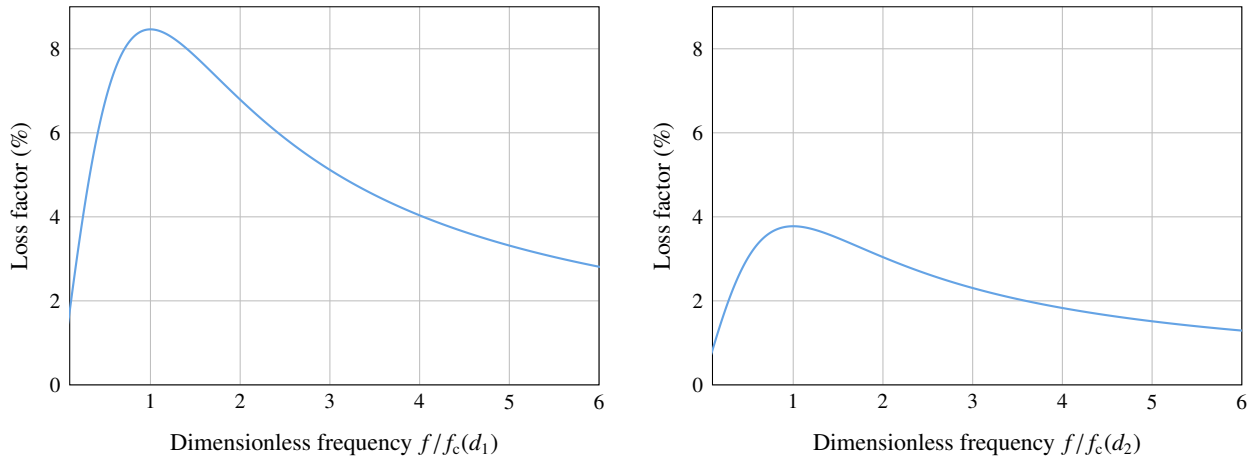

(a) $f_c(d_1) = 18\,\text{Hz}$ (b) $f_c(d_2) = 41\,\text{Hz}$

Figure 3: Global loss factor as a function of dimensionless frequency for two MPPs with constant size (490 mm × 570 mm × 1 mm) and $\phi = 10\,\%$: (a) first mode for MPP1, (b) second mode for MPP2. For both MPPs, d is set to induce maximum damping on the considered mode

and the damping will be all the more important as the first natural frequency f_{11} is low.

3. EXPERIMENTAL VALIDATIONS

Experimental measurements are performed with an Oberst test bench illustrated in Figure 4. The MPP is clamped at $x = 0$, free at $x = L_x$ and free along $y = \pm L_y/2$. The excitation of amplitude F_{ext} is provided by a magnetic exciter located at $x = L_x$ and the response is measured by a magnetic sensor at $x = S$. This set-up provides plate movements without adding extra mass and without obstructing the perforations, due to the sensors and exciters. The sample is designed with $d = 1$ mm to satisfy

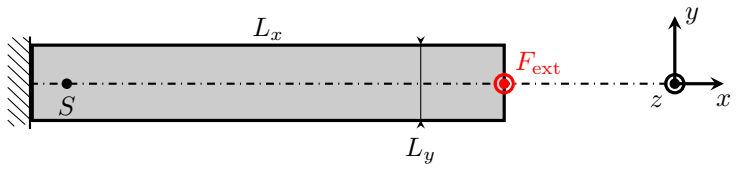

(a) Principle and dimensions

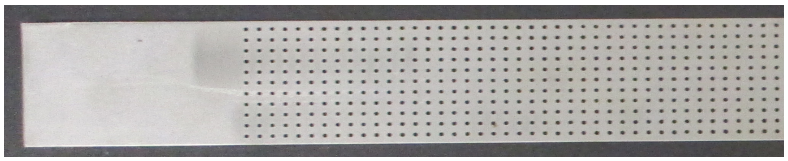

(b) Tested microperforated plate

Figure 4: Experimental set-up: the dimensions are 130 mm × 30 mm × 0.87 mm; perforation rate and perforation diameter are $d = 1$ mm and $\phi = 10\,\%$ respectively.

$f_c(d) = f_{11} = 40\,\text{Hz}$.

The mobility of the tested microperforated plate as well as the reference non-perforated plate is plotted in Figure 5. The decrease in the amplitude of the mobility of the MPP compared to that of the non-perforated plate shows the damping added by the microperforations, especially in the low frequency range. On the first peak, the gain is about 9 dB. The frequency shift is due to the ϕ-dependence of Young's modulus and solid mass density of the MPP [10]. Figure 5 also shows a good agreement between theory and measurements. The differences between measured and theoretical MPP

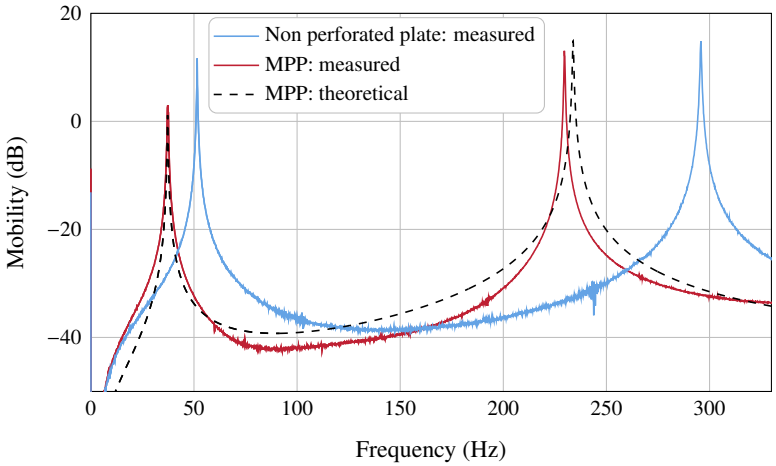

Figure 5: Mobilities for an MPP and the corresponding non-perforated plate.

are probably due to the fact that Young's modulus is independent of the frequency in the analytical model.

4. CONCLUSIONS

The objective of this work was to investigate the possibility of using microperforated plates to archive structural damping. An analytical model used to explore the vibratory responses of MPP is developed from Biot's theory of poroelasticity. Results show that MPP could be used to significantly reduce structural vibrations in the low frequency range. This effect reaches a maximum at a particular frequency defined as a function of the perforation diameter and the perforation rate. The diameter of the perforation can be adjusted so that the characteristic frequency coincides with the natural frequency of the vibration mode to be damped. The additional damping induced by the microperforations is more important in the low frequency range. Therefore, it is recommended to adjust the perforation diameter to induce maximum damping on the first MPP mode.

REFERENCES

[1] D.-Y. Maa. Potential of microperforated panel absorber. *Journal of the Acoustical Society of America*, 104:2861, 1997. DOI:10.1121/1.423870.

[2] D. Takahashi and M. Tanaka. Flexural vibration of perforated plates and porous elastic materials under acoustic loading. *Journal of the Acoustical Society of America*, 112(4):1456–1464, 2002. DOI:10.1121/1.1497624.

[3] T. Bravo, C. Maury, and C. Pinhède. Vibroacoustic properties of thin micro-perforated panel absorbers. *Journal of the Acoustical Society of America*, 132:789–798, 2012. DOI:10.1121/1.4733555.

[4] Y.Y. Lee and E.W.M. Lee. Widening the sound absorption bandwidths of flexible micro-perforated curved absorbers using structural and acoustic resonances. *International Journal of Mechanical Sciences*, 49(8):925–934, 2007. DOI:10.1016/j.ijmecsci.2007.01.008.

[5] M.A. Biot. Theory of propagation of elastic waves in a fluid-saturated porous solid. I. Low-frequency range. *Journal of the Acoustical Society of America*, 28(2):168–178, 1956. DOI:10.1121/1.1908239, OA:hal-01368666.

[6] M.A. Biot. Theory of propagation of elastic waves in a fluid-saturated porous solid. II. Higher frequency range. *Journal of the Acoustical Society of America*, 28(2):179–191, 1956. DOI:10.1121/1.1908241, OA:hal-01368668.

[7] P. Leclaire, K.V. Horoshenkov, and A. Cummings. Transverse vibration of a thin rectangular porous plate saturated by a fluid. *Journal of Sound and Vibration*, 247(1):1–18, 2001. DOI:10.1006/jsvi.2001.3656 OA:hal-01326042.

[8] N. Atalla and F. Sgard. Modeling of perforated plates and screens using rigid frame porous models. *Journal of Sound and Vibration*, 303:195–208, 2007. DOI:10.1016/j.jsv.2007.01.012, OA:hal-03623717.

[9] Y.Y. Lee, E.W.M. Lee, and C.F. Ng. Sound absorption of a finite flexible micro-perforated panel backed by an air cavity. *Journal of Sound and Vibration*, 287:227–243, 2005. DOI:10.1016/j.jsv.2004.11.024.

[10] L. Gallerand, M. Legrand, T. Dupont, and P. Leclaire. Vibration and damping analysis of a thin finite-size microperforated plate, 2022. Preprint: OA:hal-03634548.

[11] M.A. Biot and D.G. Willis. The elastic coefficients of the theory of consolidation. *Journal of Applied Mechanics*, pages 594–604, 1957. DOI:10.1115/1.4011606.

[12] A.R. Boccaccini and Z. Fan. A new approach for the Young's modulus-porosity correlation of ceramic materials. *Ceramics International*, 23, 1997. DOI:10.1016/S0272-8842(96)00033-8.